Effect of angiotensin II-induced arterial hypertension on the voltage-dependent contractions of mouse arteries

EFFECT OF ANGIOTENSIN II-INDUCED ARTERIAL HYPERTENSION ON THE VOLTAGE-DEPENDENT CONTRACTIONS OF MOUSE ARTERIES

Paul FRANSEN[a], Cor E. VAN HOVE[b], Arthur J.A. LELOUP[a], Dorien M. SCHRIJVERS[a], Guido R.Y. DE MEYER[a], Gilles W. DE KEULENAER[a]

a: University of Antwerp, Department of Pharmaceutical Sciences, Physiopharmacology, Campus Drie Eiken, T2, Universiteitsplein 1, 2610 Antwerp, Belgium

b: University of Antwerp, Faculty of Medicine & Health Sciences, Pharmacology, Campus Drie Eiken, T2, Universiteitsplein 1, 2610 Antwerp, Belgium

Short title: angiotensin II and arterial contraction

Corresponding author: Paul Fransen, University of Antwerp, Department of Pharmaceutical Sciences, Campus Drie Eiken, Physiopharmacology T2, Universiteitsplein 1, 2610 Antwerp, Belgium

telephone: 32 3 265 29 17, fax: 32 3 265 25 67, email: paul.fransen@uantwerpen.be

Word count: 6815 (including figure legends and references)

Number of figures: 7

Compliance with ethical standards:

There are no conflicts of interest and other sources of funding unlike these mentioned under acknowledgments. All research involving animals were approved by the Ethical Committee of the University of Antwerp, and the investigations conform to the Guide for the Care and Use of Laboratory Animals published by the US National Institutes of Health (NIH Publication No. 85–23, revised 1996).

Acknowledgments:

We acknowledge the support by the University of Antwerp (Grant 29887, GOA-BOF 2407) and the Fund for Scientific Research (FWO) Flanders (Grant G.0293.10N). Tail-cuff blood pressure measurements were performed by Mrs. Annie Van Weert.

Abstract

Objectives: Arterial hypertension (AHT) affects the voltage dependency of L-type Ca^{2+} channels in cardiomyocytes. We analysed the effect of angiotensin II (AngII)-induced AHT on L-type Ca^{2+} channel-mediated isometric contractions in conduit arteries.

Methods: AHT was induced in C57Bl6 mice with AngII-filled osmotic mini-pumps (4 weeks). Normotensive mice treated with saline-filled osmotic mini-pumps were used for comparison. Voltage-dependent contractions mediated by L-type Ca^{2+} channels were studied in vaso-reactive studies *in vitro* in isolated aortic and femoral arteries by using extracellular K^+ concentration-response (KDR) experiments.

Results: In aortic segments, AngII-induced AHT significantly sensitized isometric contractions induced by elevated extracellular K^+ and depolarization. This sensitization was partly prevented by normalizing blood pressure with hydralazine, suggesting is was caused by AHT rather than by direct AngII effects on aortic smooth muscle cells. The EC_{50} for extracellular K^+ obtained *in vitro* correlated significantly with the rise in arterial blood pressure induced by AngII *in vivo*. The AHT-induced sensitization persisted when aortic segments were exposed to levcromakalim or to inhibitors of basal nitric oxide release. Consistent with these observations, AngII-treatment also sensitized the vaso-relaxing effects of the L-type Ca^{2+} channel blocker diltiazem during K^+-induced contractions. Unlike aorta, AngII-treatment desensitized the isometric contractions to depolarization in femoral arteries pointing to vascular bed specific responses of arteries to hypertension.

Conclusions: AHT affects the voltage-dependent L-type Ca^{2+} channel mediated contraction of conduit arteries. This effect may contribute to the decreased vascular compliance in AHT, and explain the efficacy of Ca^{2+} channel blockers to reduce vascular stiffness and central blood pressure in AHT.

Condensed abstract

Angiotensin II-treatment sensitized isometric contractions of mouse aortic segments to depolarization and concomitant L-type Ca^{2+} channel activation. This sensitization significantly correlated with the Angiotensin II-induced rise in blood pressure and could not be fully explained by differences in resting membrane potential of vascular smooth muscle cells or in basal nitric oxide release with arterial hypertension. Therefore, it is conceivable that arterial hypertension altered the voltage-dependent properties of L-type Ca^{2+} channels. In line with this hypothesis was the higher sensitivity of hypertensive aortic segments to the L-type Ca^{2+} channel blocker diltiazem.

Key Words

cardiovascular system, vascular smooth muscle, L-type Ca^{2+} channel, isometric contraction, hypertension, angiotensin II, aorta, femoral artery

Abbreviations

AHT: arterial hypertension; AngII: angiotensin II; KDR: extracellular K^+ concentration-response; (V)SMC: (vascular) smooth muscle cell; BP: blood pressure; L-NAME: N^{Ω}-nitro-L-arginine methyl ester; NO: nitric oxide; E_{max}: maximum contraction or relaxation; EC_{50} or log IC_{50}: concentration (log concentration) exerting 50% of the maximal response

Introduction

Angiotensin II (AngII) increases the peripheral arterial resistance, causes arterial hypertension (AHT) and reduces compliance of large conduit vessels by activation of AT-1 receptors in vascular smooth muscle cells (VSMCs)[20,21]. This process involves Ca^{2+} flux through L-type Ca^{2+} channels, as shown by the inhibitory effects of $Ca_v1.2$ gene deletion and of pharmacologic L-type Ca^{2+} channel blockers in AngII-induced hypertension [12,17,22,24,32]. Interestingly, in chronic AHT, isoforms of the $Ca_v1.2$ gene are alternatively spliced, leading to a shift in the population of L-type Ca^{2+} channels towards isoforms with a different voltage-dependency [29,30]. This shift has been described to occur in cardiomyocytes, but it is not known whether it also occurs in VSMCs and if this eventually leads to a changed vascular affinity for L-type Ca^{2+} channel blockers, which might have important consequences for their application in the treatment of AHT.

We have recently shown that VSMCs of mice conduit vessels display a continuous baseline Ca^{2+} influx via L-type Ca^{2+}channels. This Ca^{2+} influx occurred at a window of membrane potentials where activation and inactivation curves of the L-type Ca^{2+}channels overlap, leading to a so-called “window current induced contraction curve” [7,8]. Hence, the window current induced contraction curve may be considered as a physiologic reflection of the voltage-dependency of the L-type Ca^{2+}channels expressed in SMCs of the blood vessel. Because it has been reported that the expression levels and the electrophysiological properties of L-type Ca^{2+} channels change with hypertension [19,19,30,39], it was hypothesized that the swap of the different isoforms with hypertension and the concomitant swap of electrophysiological properties, are reflected in different window current induced contraction curves in the multicellular aorta of AngII-induced hypertension. Apart from eliciting altered contraction, the degree of this Ca^{2+} influx may influence the efficacy of nitric oxide (NO) to relax the vessel. Indeed, in mouse aorta the efficacy of NO to induce vasorelaxation was decreased when contractions were predominantly elicited via L-type Ca^{2+} influx[33]. Basal Ca^{2+} influx as well as basal NO

release contribute to compliance of conduit vessels [1,27] and both seem to be changed during AHT [14,40].

In the present study, we analyzed window current induced contraction curves of conduit vessels of mice with AngII-induced AHT, and hypothesized that the window current induced contraction curves would shift due to changing voltage gating features of the L-type Ca^{2+} channels. Alternative causes of such shifts of the window current induced contraction curves, including reduced NO activity and changes of the VSMCs resting membrane potential, were also analyzed. Given previous observations that proximal and distal conduit vessels react differently to angiotensin II [28,43,44], we also compared effects of AngII-induced AHT in the thoracic aorta and femoral artery.

Material and methods

AngII-induced AHT model

Male C57Bl/6 mice were treated with saline (n=10) or with AngII (n=17) via subcutaneous osmotic minipumps (model 1004, Alzet, Cupertino, CA) for 4 weeks (1000 $ng.kg^{-1}.day^{-1}$). Pumps were implanted subcutaneously on the back between the shoulder blades and hips while animals were anesthetized by inhalation of sevoflurane. To counteract AHT by AngII-treatment some mice (n=5) received 200 mg/ml hydralazine in the drinking water, starting one week before implantation of the AngII-diluting minipumps.

The studies were approved by the Ethical Committee of the University of Antwerp, and the investigations conform to the Guide for the Care and Use of Laboratory Animals published by the US National Institutes of Health (NIH Publication No. 85–23, revised 1996).

Blood pressure measurements

Systolic and diastolic blood pressure (BP) were recorded weekly by the tail-cuff method. Animals were put in a heating ($37^{o}C$) chamber and restraint in a Plexiglas cage to which the animals had been previously conditioned. A pneumatic pulse sensor was attached to the tail distal to an occluding cuff controlled by a Programmed Electro-Sphygmomanometer (Narco Bio-Systems, Austin, TX). Voltage output from the cuff and the pulse sensor were recorded and analyzed by a PowerLab signal transduction unit and associated Chart software (ADInstruments, Colorado Springs, CO). At least three to five separate pressure measurements were averaged from each animal on each recording day. After 4 weeks of training sessions, necessary for the mice to become accustomed to the tail-cuff procedure, sessions of recorded measurements were then made by a single investigator between 9 and 12 AM daily.

Vascular reactivity

Animals were euthanized by perforating the diaphragm under pentobarbital anaesthesia (sodium pentobarbital, 75 mg kg^{-1}, i.p.). The thoracic aorta and the femoral artery were carefully removed, stripped of adherent tissue and dissected systematically. Segments (vessel width ± 2 mm) were immersed in Krebs Ringer solution (KR 37°C, 95% O_2/5% CO_2, pH 7.4) with (in mM): NaCl 118, KCl 4.7, $CaCl_2$ 2.5, KH_2PO_4 1.2, $MgSO_4$ 1.2, $NaHCO_3$ 25, CaEDTA 0.025, and glucose 11.1. High K^+- solutions were prepared by replacing NaCl with equimolar KCl.

Aortic segments were mounted in 10 ml organ baths. Tension was measured isometrically with a Statham UC2 force transducer (Gould) connected to a data acquisition system (Powerlab 8/30, ADInstruments, Spechbach, Germany) as described [30]. Segments were gradually stretched until a stable loading tension of 16 mN, the optimal preload to attain maximal force development by 50 mM K^+. Isometric force was reported in mN. When necessary, NO formation was inhibited with 300 μM N^{Ω}-nitro-L-arginine methyl ester (L-NAME) and to avoid any vasomotor interference due to prostanoids, 10 μM indomethacin was added to all solutions.

Femoral artery segments (vessel width ± 2 mm) were mounted in a wire (40 μm) myograph (DMT, Denmark). After a short equilibration period of 30 minutes, the segments were gradually stretched until wall stress attained values above 13.3 kPa (100 mm Hg). Segments were then set at the internal circumference according to 90% of the 13.3 kPa stress, after which all transducers were re-set to zero force in order to measure active force. Contractile force was measured and reported in mN mm^{-1}. Also here, NO formation could be inhibited with 300 μM L-NAME and prostanoid release with 10 μM indomethacin.

To measure window current induced contraction curves voltage clamp protocols as used in electrophysiological studies were simulated by elevating extracellular K^+ concentration. The holding potential from which voltage steps would be applied was

mimicked by holding the segments at each K^+ concentration before a subsequent challenge with higher K^+ (cumulative depolarisation)[8]. To compensate for resting membrane potential differences between segments of different animals and of different experimental groups, in some experiments, 1 µM levcromakalim, an ATP-dependent K^+ channel opener, was applied at the start of the K^+-clamp experiments [7]. After attaining maximal contractions with 50 or 124 mM K^+, relaxations were induced with increasing concentrations of diltiazem ($3*10^{-9}$ – $3*10^{-5}$M).

Calcium measurements

An aortic segment (1.5 mm in length) was mounted in a wire myograph (Danish Myo Technology, Gainesville, FL, USA) above an inverted microscope (Carl Zeiss, Zaventem, Belgium). To avoid endothelial calcium signals, the endothelium was removed by rubbing the interior of the segment with a braided silk wax. The segment was loaded for 2 h with 10 µM Fura-2 AM (Teflabs, Austin, TX, USA) in KR solution supplemented with 1 mg/ml BSA (Sigma-Aldrich) and 0.02% Pluronic® F-127 (Sigma-Aldrich) at room temperature while being aerated by 95% O_2/5% CO_2. Subsequently, the temperature was raised to 37°C and the segment was set to its optimal preload. The emission (510 nm) ratio at dual excitation (340 and 380 nm) was used as a relative measure of free intracellular calcium (relative units, RU) after subtraction of background emission values, which were determined by adding 2 mM $MnCl_2$ (Sigma-Aldrich) at the end of each experiment.

Data analysis

All results are expressed as mean±s.e.m. with n representing the number of mice. Concentration-response curves were fitted with sigmoidal dose-response equations with variable slope, which revealed maximum contraction or relaxation (E_{max}) and (the logarithm of) the concentration resulting in 50% of the maximal response (EC_{50} or log IC_{50}) for each vessel segment. Window current induced contraction curves were constructed as

the first K^+ derivative of the K^+ dose-response curves (dF (mN or %)/dK^+ (mM)[7]). One-way ANOVA, two-way ANOVA with Bonferonni's multiple comparison post-test or unpaired *t*-test were performed using GraphPad Prism, version 6 (GraphPad Software, San Diego California USA) to compare means of the different experimental groups. A 5% level of significance was selected. Two-tailed Spearman correlation (nonparametric correlation, Graphpad Prism) with Spearman r (Sr) and p were analyzed from XY tables, with X, systolic BP and Y, log(IC_{50}) of diltiazem or EC_{50} of extracellular K^+.

Results

1. AngII-treatment causes AHT

The mean arterial BP after 4 weeks of AngII treatment increased from 133±8 to 167±4 mm Hg (n=10-17, p<0.001, Fig. 1). During co-treatment of AngII with hydralazine the AngII-induced hypertension was prevented and BP was 129±11 mm Hg (n=5, p<0.01 versus AngII).

2. AngII-induced AHT shifts the aortic window current induced contraction curves and increases K^+ sensitivity.

Window current induced contraction curves in aortic segments were determined by exposure to extracellular K^+ (Fig. 2) [7,8]. Maximal contractions, attained at 40 to 50 mM K^+, were significantly larger in segments of AngII-treated mice versus control mice (E_{max}: 16.7±0.9 mN, n=12, versus 12.8±1.1 mN, n=6, P<0.05, Fig. 2c). Moreover, also intracellular Ca^{2+} was elevated in VSMCs of AngII-treated mice as well in basal conditions as after depolarization of the aortic segments with 30 mM K^+ (Fig. 2e). As shown in Figs 2a and b, segments of AngII-treated mice were significantly more sensitive to the extracellular K^+ concentration than control mice and EC_{50} decreased from 31.9±0.3 (n=6) to 25.8±0.8 mM (n=12, P<0.001). Accordingly, the window current induced contraction curve (Fig. 2b), the peak of which coincides with the EC_{50} for extracellular K^+ concentration, was shifted by 6 mM in the direction of lower K^+.

3. Inhibition of basal NO release synthesis attenuates, but does not eliminate the AngII-induced shift of the aortic window current induced contraction curve.

Mice with AngII-induced AHT have been described to display endothelial dysfunction [23]. Because this might result in a reduction of the hyperpolarizing effect of NO on the VSMCs [2,6], this would shift the window current induced contraction curves to lower K^+ concentrations without affecting the functional properties of the L-type Ca^{2+}

channels [7]. In order to exclude that the shift of the window current induced contraction curves in aortic segments of mice with AngII-induced AHT was due to attenuated NO availability and the subsequent depolarization of VSMCs, aortic segments from saline- and AngII-treated mice were studied before and after inhibition of basal NO release with 300 µM L-NAME **(Fig. 2d).**

First, as expected, L-NAME significantly shifted the window current induced contractions to lower K^+ in both experimental groups. This shift was significantly larger in saline-treated (-7.1±0.6 mM, n=6) than in AngII-treated animals (-4.2±0.4 mM, n=18, $p<0.01$), consistent with endothelial dysfunction and impaired NO availability in mice with AngII-induced AHT. However, even in the presence of L-NAME, the window current induced contraction curves of AngII-treated animals remained significantly shifted to the left compared with control animals. This observation indicates that NO-mediated changes of membrane potential are not sufficient to explain the shifts of the curves induced by AngII-treatment. It should be noted that endothelial function, as assessed by acetylcholine-induced relaxation, and smooth muscle cell sensitivity to NO, as assessed by diethylamine NO (DEANO)-induced relaxation, were not affected by AngII-treatment (Table 1).

4. Hyperpolarization of aortic segments with levcromakalim attenuates, but does not eliminate the AngII-induced shift of the aortic window current induced contraction curve.

In order to exclude other, NO-independent mediated changes of membrane potential as a cause of shifted window current induced contraction curves in aortic segments of mice with AngII-induced AHT, the curves were determined in the presence of 1 µM levkromakalim **(Fig. 2f).** This substance opens ATP-dependent K^+ channels, and hyperpolarizes the resting membrane potential of VSMC to the K^+-equilibrium potential [7,15], thereby equalizing the membrane potentials of all aortic preparations.

First, according to levcromakalim´s action, the K^+-contraction curves shifted to higher K^+ concentrations. Consistent with the L-NAME-effects, the levcromakalim-induced shift of the curves was significantly larger in AngII-treated than in control segments (respectively +7.4±0.5 mM, n=18; and +5.1±0.7 mM, n=6, $p<0.05$). Second, in the presence of levcromakalim, window current induced contraction curves of aortic segments from AngII-treated mice remained significantly shifted to the left compared with segments from saline-treated mice. This indicates that differences in resting membrane potential are not sufficient to explain the shifts in the window current induced contraction curves.

5. Equal time-dependent shifts of the window current induced contraction curves for saline- and AngII-treated mice.

In saline- and AngII-treated animals, contractions at different K^+ were measured at 3 minutes, when Ca^{2+} signals attained steady-state and at 15 minutes, when sensitization increased force further without change in Ca^{2+} [8] (Fig. 3). As expected, sensitization shifted the window current induced contraction curves to lower K^+, but the shift of the window current induced contraction curve (red and green arrow in figure 3) in AngII- compared with saline-treated animals was the same at 3 and 15 minutes. This indicated that AngII-treatment mainly affected the L-type Ca^{2+} influx (compare with Fig. 2c) and had only minor effects on subsequent sensitization.

6. AngII-treatment increases aortic sensitivity to the L-type Ca^{2+} channel blocker diltiazem

Above experiments suggest that AngII-induced AHT changes the functional properties of the L-type Ca^{2+} channels in aortic VSMCs. To further prove this possibility, relaxing effects of the L-type Ca^{2+} channel blocker diltiazem ($3*10^{-9}$-$3*10^{-5}$ M) were measured after attaining steady-state contractions with 124 mM K^+ in the presence of L-NAME. Although diltiazem completely inhibited the contraction by 124 mM K^+ in both

experimental groups, aortic segments of AngII-treated mice displayed a significantly higher sensitivity for diltiazem (Fig. 4a, Table 2).

7. Hydralazine partly reverses the AngII-induced shift of the aortic window current induced contraction curve.

Subsequently, we studied whether either AngII or alternatively the increase in BP induced the shift of the window current induced contraction curves. As shown in Fig. 1, hydralazine counteracted AngII-induced AHT. Figs. 4b shows K^+-contraction curves for aortic segments of control, AngII-treated and AngII + hydralazine-treated mice. The leftward shift of the curves for the AngII-treated mice was partly prevented by hydralazine. The higher sensitivity of aortic segments of AngII-treated mice to the L-type Ca^{2+} channel blocker, diltiazem, was completely reversed by co-treatment with hydralazine (Fig. 4a) and also the shift of the curves with NO-inhibition was partly reversed by hydralazine co-treatment (data not shown). These data indicate that at physiologic membrane potentials of -65 to -35 mV [7], the effects of AngII-treatment on voltage-dependent contractions via L-type Ca^{2+} channels are explained by its effect on arterial BP.

8. Relationship between BP and K^+- or diltiazem-sensitivity

Given the causal relationship between arterial BP and the voltage-dependent properties of aortic L-type Ca^{2+} channels, we plotted individual data for *in vivo* arterial systolic BP of each mouse against the *in vitro* log(IC_{50}) of the aorta-dilating effect of diltiazem (Fig. 4c) or against its corresponding *in vitro* aortic EC_{50} for extracellular K^+ (Fig. 4d). Both plots show a significant correlation. With increasing BP the sensitivity to aortic dilation by diltiazem and to aortic VSMC depolarization and contraction by extracellular K^+ was higher.

9. Femoral artery segments display decreased K^+ sensitivity with AngII-treatment

Given previous observations that proximal and distal conduit vessels react differently to AngII [28,43,44], window current induced contraction curves were also measured in segments of the femoral artery. As in the thoracic aorta, maximal force induced by 50 mM K^+ was significantly larger for AngII-treated versus control animals (5.38±0.16 versus 4.52±0.20 mN/mm). Remarkably, and opposite to thoracic aortic segments, femoral artery segments of AngII-treated mice became less sensitive to extracellular K^+. Thereby, EC_{50} increased from 21.6±0.5 to 25.1±1.6 mM ($P<0.001$) and the window current induced contraction curve shifted by 3.5 mM to higher K^+ (Fig. 5).

In addition, L-NAME did not affect contractions of femoral artery segments in saline- or AngII-treated segments, indicating that basal NO release in femoral artery was absent (data not shown). Levcromakalim shifted both window current induced contraction curves to the left by 2.1±0.5 mM in control and 3.5±0.4 mM ($p=0.07$, $n=6$) in AngII-treated segments. These shifts were smaller than in aortic segments ($P<0.01$ control and $P<0.001$ AngII-infused). Similarly as observed in aortic segments, even after normalization with levcromakalim for different resting potentials, vascular segments of AngII-treated mice were significantly less sensitive to depolarization than control segments.

10. Direct effects of AngII in aortic and femoral artery segments

AngII concentration-response experiments were measured in thoracic aorta and femoral artery in non-treated C57Bl6 mice (Fig. 6). At normal K^+, AngII reached maximal effects of 4.7±0.5 mN/mm or 74.3±12.7% of the 50 mM K^+ contraction with an EC_{50} of 5.64 ±0.79 nM in femoral artery, but was without any effect in aorta (n=4). The. Pre-treatment of femoral artery and aortic segments with 20 mM K^+ or 27.5 mM K^+, respectively, (K^+ concentrations which elicited 20-25% contraction) failed to increase the sensitivity of aorta to AngII, but slightly increased the efficacy (E_{max}: 6.1±0.8 mN/mm or 82.4±15.1% of the 50 mM K^+ contraction with EC_{50} of 2.41±0.16 nM) in femoral artery. This contraction was sensitive to diltiazem (not shown).

Discussion

The main result of the present study is that AngII-induced AHT increased and sensitized the voltage-dependent contractions of mice aortic segments depolarized by extracellular K^+. This results in a higher sensitivity of aortic segments to the relaxing effects of the L-type Ca^{2+} channel blocker diltiazem. The effects occurred in parallel with, but independently from, a shift in the resting membrane potential of the VSMC. The latter shift in membrane potential was, at least partly, induced by reduced basal NO bio-availability in the vessel wall.

Endothelial dysfunction is a common feature in AHT [23], leading to impaired NO synthesis and/or bioavailability [3,13,35,36,42]. We did, however, not find evidence for attenuated NO release evoked by acetylcholine or sensitivity of the VSMCs for exogenous NO. Because basal and stimulated NO release are probably differently regulated[34], this does not preclude attenuated basal NO efficacy. In line with our previous observation that basal NO release from endothelial cells of mouse aorta shifted the window current induced contraction curve in the repolarizing direction [7], inhibition of basal NO release shifted the window current induced contraction curve in aorta to lower K^+ concentrations in the present study. The shift was significantly larger in control (-7.1 mM K^+) and AngII + hydralazine (-5.5 mM K^+, data not shown) than in AngII-treated animals (-4.2 mM K^+), indicating that basal endothelial NO release in aortas of hypertensive animals was indeed attenuated.

Both in AngII [6] and in other hypertensive models [2,40], AHT is associated with depolarized membrane potentials of the VSMC. This depolarization may be due to attenuated basal NO release and (partial) removal of the hyperpolarizing effect of NO [2]. After elimination of basal NO release with L-NAME or after hyperpolarization of the VSMC to the K^+ equilibrium potential with levcromakalim, which does not affect the voltage-dependent properties of L-type Ca^{2+} channels [7,8], window current induced contraction curves were still significantly shifted with AHT. This finding indicated that shifts of the

window current induced contraction curves with hypertension were not only due to depolarized resting potentials of VSMCs, but probably reflect shifts in the voltage-dependence of L-type Ca^{2+} channels. Also in the femoral artery, which lacks basal eNOS activity [5], hyperpolarization of the VSMCs with levcromakalim could not prevent the shift of the window current induced contraction to higher K^+ with hypertension, suggesting that in the hypertensive femoral artery shifts in the Ca^{2+} channel population occur.

Isometric contractions of arteries induced by elevated extracellular K^+ are exclusively mediated by L-type Ca^{2+} influx and are therefore completely inhibited by L-type Ca^{2+} channel blockers [8]. In most hypertensive models, including the spontaneously hypertensive rat, L-type Ca^{2+} channel expression and activity increases and voltage-dependent properties are affected [39,9,25,26,38,40,4], which is consistent with the increased maximal isometric contraction, altered window current induced contraction curves and intracellular Ca^{2+} concentration with hypertension in AngII-treated mice in this study. In the cardiovascular system, numerous alternatively spliced isoforms of L-type Ca^{2+} channels occur, which leads to a non-homogeneous population of channels [16]. In addition, the channel population appears to be flexible and to adapt during different pathophysiological conditions including AHT and other [9,25,26,31,39,38,37,40]. We hypothesize that changes in $Ca_v1.2$ channel populations is the molecular basis for the observations in this study. For example, $Ca_v1.2$ channels in cardiac myocytes and smooth muscle cells differ at four alternatively spliced sites: exon 1/1a, exon 8/8a, exon 9*, and exon 31/32 [18]. Notably, the VSMC-specific $Ca_v1.2$ splice variant, $Ca_v1.2$SM (1/8/9*/32/Δ33) displays a hyperpolarized window current and an enhanced state-dependent block by nifedipine, when compared with the predominant cardiac isoform, $Ca_v1.2$CM (1a/8a/Δ9*/32/33). This phenomenon is a presumed explanation of the different cardiac and vascular sensitivity to L-type Ca^{2+} channel blockers. Hence, if AHT affects the voltage-dependent gating of L-type Ca^{2+} channels, as shown in mesenteric arteries of spontaneous hypertensive rats, which displayed higher abundance of exon9*

transcripts[4], it should also affect the window L-type Ca^{2+} influx and related contraction, which was suggested in the present study by the higher affinity for the L-type Ca^{2+} channel blocker diltiazem. Although the results of the present study indicate that arterial hypertension may affect voltage-dependent properties of L-type Ca^{2+} channels, the regulation of these properties in AngII-induced AHT in mice may involve other regulatory intracellular mechanisms [41,10].

Although AngII- induced AHT increased the maximal isometric contractions induced by depolarization in aortic and femoral segments, the effects of AHT on the voltage-dependent window current induced contraction curves were different between both vessel types. The AngII-induced changes in the window current induced contraction curves may, however, reflect direct or indirect effects of AngII on L-type Ca^{2+} channels. Similar to our observations in aorta and femoral artery, it has been described that the direct contractile response of thoracic and abdominal aorta, carotid artery and femoral artery to the application of AngII were completely different: with 60 mM K^+ contraction set to 100%, AngII caused contractions of 75% in abdominal aorta, 76% in femoral artery, but only 24% in carotid artery and 3.5% in thoracic aorta. In abdominal aorta, the EC_{50} was 4.6 nM [44,43]. In view of the previously observed high expression of AT1b receptors in femoral artery and the low expression in aorta [28,43,44], it may be assumed that the decrease in sensitivity to depolarization in the femoral artery may, therefore, be related to the direct effects of AngII on femoral artery. This may be a local protective mechanism to prevent strong AngII-induced constrictions of the smaller blood vessels during prolonged AngII-infusion. On the other hand, the increase in sensitivity to depolarization in the aorta, which is also observed in rat aorta from NOS inhibition-induced hypertensive rats [11], is probably merely due to the hypertensive effect of AngII rather than to direct AngII effects on the aortic VSMC. The significant correlation between the *in vivo* systolic BP and the *in vitro* aortic EC_{50} for extracellular K^+ or the *in vitro* log(IC_{50}) of the aorta-dilating effect of diltiazem and the partial counteraction by hydralazine of the AngII-induced shifts of the

window current induced contraction curves in aorta suggest that hypertension and not AngII directly affects vascular biology of aortic L-type Ca^{2+} channels.

In summary, in the present study we showed that during AngII-induced AHT the increase in voltage-sensitivity of the hypertensive aorta was due to the depolarized resting membrane potential of the VSMC, the reduced efficacy of basal NO release and the altered properties of the L-type Ca^{2+} channels as evidenced by the higher sensitivity to the L-type Ca^{2+} channel blocker diltiazem. These events, together with altered passive properties of the conduit arteries in hypertension, may be at the basis of the decreased vascular compliance in AHT. They may also explain the high efficacy of Ca^{2+} channel blockers to improve vascular compliance and to decrease central blood pressure in hypertension [17].

References

1. Bellien J, Favre J, Iacob M, Gao J, Thuillez C, Richard V, Joannides R (2010) Arterial stiffness is regulated by nitric oxide and endothelium-derived hyperpolarizing factor during changes in blood flow in humans. Hypertension 55:674-680

2. Bratz IN, Falcon R, Partridge LD, Kanagy NL (2002) Vascular smooth muscle cell membrane depolarization after NOS inhibition hypertension. Am J Physiol Heart Circ Physiol 282:H1648-H1655

3. Choi H, Allahdadi KJ, Tostes RC, Webb RC (2011) Augmented S-nitrosylation contributes to impaired relaxation in angiotensin II hypertensive mouse aorta: role of thioredoxin reductase. J Hypertens 29:2359-2368

4. Cox RH, Fromme S (2015) Expression of Calcium Channel Subunit Variants in Small Mesenteric Arteries of WKY and SHR. Am J Hypertens (2015) doi: 10.1093/ajh/hpv024

5. Crauwels HM, Van Hove CE, Herman AG, Bult H (2000) Heterogeneity in relaxation mechanisms in the carotid and the femoral artery of the mouse. Eur J Pharmacol 404:341-351

6. Dal-Ros S, Bronner C, Schott C, Kane MO, Chataigneau M, Schini-Kerth VB, Chataigneau T (2009) Angiotensin II-induced hypertension is associated with a selective inhibition of endothelium-derived hyperpolarizing factor-mediated responses in the rat mesenteric artery. J Pharmacol Exp Ther 328:478-486

7. Fransen P, Van Hove C, van Langen J, Bult H (2012) Contraction by Ca^{2+} influx via the L-type Ca^{2+} channel voltage window in mouse aortic segments is modulated by nitric oxide. In: Sugi H (editor) Current basic and pathological approaches to the function of muscle cells and tissues-From molecules to Humans Rijeka, Croatia: Intech (www intech com)69-92

8. Fransen P, Van Hove CE, van Langen J., Schrijvers DM, Martinet W, De Meyer GR, Bult H (2012) Contribution of transient and sustained calcium influx, and sensitization to depolarization-induced contractions of the intact mouse aorta. BMC Physiol 12:9:doi:10.1186/1472-6793-12-9-

9. Hermsmeyer K, Rusch NJ (1989) Calcium channel alterations in genetic hypertension. Hypertension 14:453-456

10. Hofmann F, Flockerzi V, Kahl S, Wegener JW (2014) L-type CaV1.2 calcium channels: from in vitro findings to in vivo function. Physiol Rev 94:303-326

11. Kanagy NL (1997) Increased vascular responsiveness to alpha 2-adrenergic stimulation during NOS inhibition-induced hypertension. Am J Physiol 273:H2756-H2764

12. Kanaide H, Ichiki T, Nishimura J, Hirano K (2003) Cellular mechanism of vasoconstriction induced by angiotensin II: it remains to be determined. Circ Res 93:1015-1017

13. Kane MO, Etienne-Selloum N, Madeira SV, Sarr M, Walter A, Dal-Ros S, Schott C, Chataigneau T, Schini-Kerth VB (2010) Endothelium-derived contracting factors mediate the Ang II-induced endothelial dysfunction in the rat aorta: preventive effect of red wine polyphenols. Pflugers Arch 459:671-679

14. Kisters K, Wessels F, Kuper H, Tokmak F, Krefting ER, Gremmler B, Kosch M, Barenbrock M, Hausberg M (2004) Increased calcium and decreased magnesium concentrations and an increased calcium/magnesium ratio in spontaneously hypertensive rats versus Wistar-Kyoto rats: relation to arteriosclerosis. Am J Hypertens 17:59-62

15. Knot HJ, Nelson MT (1998) Regulation of arterial diameter and wall [Ca^{2+}] in cerebral arteries of rat by membrane potential and intravascular pressure. J Physiol 508 (Pt 1):199-209

16. Koch WJ, Ellinor PT, Schwartz A (1990) cDNA cloning of a dihydropyridine-sensitive calcium channel from rat aorta. Evidence for the existence of alternatively spliced forms. J Biol Chem 265:17786-17791

17. Koumaras C, Tzimou M, Stavrinou E, Griva T, Gossios TD, Katsiki N, Athyros VG, Mikhailidis DP, Karagiannis A (2012) Role of antihypertensive drugs in arterial 'de-stiffening' and central pulsatile hemodynamics. Am J Cardiovasc Drugs 12:143-156

18. Liao P, Yu D, Li G, Yong TF, Soon JL, Chua YL, Soong TW (2007) A smooth muscle $Ca_v1.2$ calcium channel splice variant underlies hyperpolarized window current and enhanced state-dependent inhibition by nifedipine. J Biol Chem 282:35133-35142

19. Liao P, Yu D, Lu S, Tang Z, Liang MC, Zeng S, Lin W, Soong TW (2004) Smooth muscle-selective alternatively spliced exon generates functional variation in $Ca_v1.2$ calcium channels. J Biol Chem 279:50329-50335

20. Mahmud A, Feely J (2004) Arterial stiffness and the renin-angiotensin-aldosterone system. J Renin Angiotensin Aldosterone Syst 5:102-108

21. McFarlane SI, Kumar A, Sowers JR (2003) Mechanisms by which angiotensin-converting enzyme inhibitors prevent diabetes and cardiovascular disease. Am J Cardiol 91:30H-37H

22. Moosmang S, Schulla V, Welling A, Feil R, Feil S, Wegener JW, Hofmann F, Klugbauer N (2003) Dominant role of smooth muscle L-type calcium channel $Ca_v1.2$ for blood pressure regulation. EMBO J 22:6027-6034

23. Nakashima H, Suzuki H, Ohtsu H, Chao JY, Utsunomiya H, Frank GD, Eguchi S (2006) Angiotensin II regulates vascular and endothelial dysfunction: recent topics of Angiotensin II type-1 receptor signaling in the vasculature. Curr Vasc Pharmacol 4:67-78

24. Navedo MF, Nieves-Cintron M, Amberg GC, Yuan C, Votaw VS, Lederer WJ, McKnight GS, Santana LF (2008) AKAP150 is required for stuttering persistent Ca2+ sparklets and angiotensin II-induced hypertension. Circ Res 102:e1-e11

25. Ohya Y, Tsuchihashi T, Kagiyama S, Abe I, Fujishima M (1998) Single L-type calcium channels in smooth muscle cells from resistance arteries of spontaneously hypertensive rats. Hypertension 31:1125-1129

26. Rusch NJ, Hermsmeyer K (1988) Calcium currents are altered in the vascular muscle cell membrane of spontaneously hypertensive rats. Circ Res 63:997-1002

27. Safar M, Chamiot-Clerc P, Dagher G, Renaud JF (2001) Pulse pressure, endothelium function, and arterial stiffness in spontaneously hypertensive rats. Hypertension 38:1416-1421

28. Swafford AN, Jr., Harrison-Bernard LM, Dick GM (2007) Knockout mice reveal that the angiotensin II type 1B receptor links to smooth muscle contraction. Am J Hypertens 20:335-337

29. Tang ZZ, Hong X, Wang J, Soong TW (2007) Signature combinatorial splicing profiles of rat cardiac- and smooth-muscle $Ca_v1.2$ channels with distinct biophysical properties. Cell Calcium 41:417-428

30. Tang ZZ, Liao P, Li G, Jiang FL, Yu D, Hong X, Yong TF, Tan G, Lu S, Wang J, Soong TW (2008) Differential splicing patterns of L-type calcium channel $Ca_v1.2$ subunit in hearts of Spontaneously Hypertensive Rats and Wistar Kyoto Rats. Biochim Biophys Acta 1783:118-130

31. Tiwari S, Zhang Y, Heller J, Abernethy DR, Soldatov NM (2006) Atherosclerosis-related molecular alteration of the human $Ca_v1.2$ calcium channel alpha1C subunit. Proc Natl Acad Sci U S A 103:17024-17029

32. Ushio-Fukai M, Yamamoto H, Toyofuku K, Nishimura J, Hirano K, Kanaide H (2000) Changes in the cytosolic Ca2+ concentration and Ca(2+)-sensitivity of the contractile apparatus during angiotensin II-induced desensitization in the rabbit femoral artery. Br J Pharmacol 129:425-436

33. Van Hove CE, Van der Donckt C, Herman AG, Bult H, Fransen P (2009) Vasodilator efficacy of nitric oxide depends on mechanisms of intracellular calcium mobilization in mouse aortic smooth muscle cells. Br J Pharmacol 158:920-930

34. van Langen J, Fransen P, Van Hove CE, Schrijvers DM, Martinet W, De Meyer GR, Bult H (2012) Selective loss of basal but not receptor-stimulated relaxation by endothelial nitric oxide synthase after isolation of the mouse aorta. Eur J Pharmacol 696:111-119

35. Virdis A, Neves MF, Amiri F, Touyz RM, Schiffrin EL (2004) Role of NAD(P)H oxidase on vascular alterations in angiotensin II-infused mice. J Hypertens 22:535-542

36. Wang D, Chabrashvili T, Borrego L, Aslam S, Umans JG (2006) Angiotensin II infusion alters vascular function in mouse resistance vessels: roles of O and endothelium. J Vasc Res 43:109-119

37. Wang J, Thio SS, Yang SS, Yu D, Yu CY, Wong YP, Liao P, Li S, Soong TW (2011) Splice variant specific modulation of CaV1.2 calcium channel by galectin-1 regulates arterial constriction. Circ Res 109:1250-1258

38. Wang W, Pang L, Palade P (2011) Angiotensin II upregulates Ca(V)1.2 protein expression in cultured arteries via endothelial H(2)O(2) production. J Vasc Res 48:67-78

39. Wang WZ, Saada N, Dai B, Pang L, Palade P (2006) Vascular-specific increase in exon 1B-encoded CAV1.2 channels in spontaneously hypertensive rats. Am J Hypertens 19:823-831

40. Wellman GC, Cartin L, Eckman DM, Stevenson AS, Saundry CM, Lederer WJ, Nelson MT (2001) Membrane depolarization, elevated Ca(2+) entry, and gene expression in cerebral arteries of hypertensive rats. Am J Physiol Heart Circ Physiol 281:H2559-H2567

41. Wynne BM, Chiao CW, Webb RC (2009) Vascular Smooth Muscle Cell Signaling Mechanisms for Contraction to Angiotensin II and Endothelin-1. J Am Soc Hypertens 3:84-95

42. Wynne BM, Labazi H, Tostes RC, Webb RC (2012) Aorta from angiotensin II hypertensive mice exhibit preserved nitroxyl anion mediated relaxation responses. Pharmacol Res 65:41-47

43. Zhou Y, Chen Y, Dirksen WP, Morris M, Periasamy M (2003) AT1b receptor predominantly mediates contractions in major mouse blood vessels. Circ Res 93:1089-1094

44. Zhou Y, Dirksen WP, Babu GJ, Periasamy M (2003) Differential vasoconstrictions induced by angiotensin II: role of AT1 and AT2 receptors in isolated C57BL/6J mouse blood vessels. Am J Physiol Heart Circ Physiol 285:H2797-H2803

Fig. 1 Mean arterial blood pressure in control mice (n=10), AngII-infused mice (n=17) and AngII-infused mice treated with hydralazine (n=5).***: p<0.001 AngII versus control; ##: p<0.01: AngII + hydralazine (H) versus AngII

Fig. 2 Effect of extracellular K^+ on isometric contractions of aortic segments of saline (n=6)- and AngII (n=17)-treated mice. a K^+ concentration-force curves for aortic segments in control (open circles) and following AngII-treatment (red, solid circles). b Window current induced contraction curves were constructed by plotting the change of force (%) per mM change of extracellular K^+. The dashed lines indicate the EC_{50} in the absence of eNOS blockers and are also indicated in d and f. c Maximal contractions induced by 50 mM K^+ in saline- and AngII-treated mice. d Window current induced contraction curves following inhibition of basal NO release with 300 µM L-NAME (squares). For comparison, the arrows on top of the figure (black for control and red for AngII) indicate the EC_{50}-shifts induced by adding L-NAME. e Intracellular VSMC Ca^{2+} concentration (ratio 340/380 in RU) in saline (white, n=3)- and AngII (red, n=6)-treated aortic segments in basal (open bars) conditions and following depolarization with 30 mM K^+ (dotted bars). f Window current induced contraction curves in the presence of 1 µM levcromakalim (diamonds). For comparison, the arrows on top of the figure (black for control and red for AngII) indicate the EC_{50}-shifts induced by adding levcromakalim. *, **, ***: P<0.05, 0.01, 0.001 AngII versus control

Fig. 3 Time-dependent shifts of the window current induced contraction curves for saline- and AngII-treated mice. Contractions by cumulative increase of extracellular K^+ were measured in saline-treated (saline, n=6) and AngII-treated (AngII, n=12) mice 3 minutes (3') and 15 minutes (15') after increasing the extracellular K^+ concentration in the presence of L-NAME. Arrows indicate the shifts with AngII-treatment of the window

current induced contraction curves measured after 3' and 15' and these shifts were similar.

Fig. 4 Effects of hydralazine treatment on relative KDR curves (a) and maximal effects (b, E_{max}, mN) in saline- (open circles, white, n=6), AngII-treated (solid circles, red, n= 12) and AngII-treatment in combination with hydralazine (AngII + H, solid circles, black, n=5). a: *, **, ***: P<0.05, 0.01, 0.001 AngII versus saline; $, $$$: P<0.05, 0.01 AngII + H versus AngII; #, ###: P<0.05, 0.001 AngII + H versus saline, b: *: P<0.05 AngII or AngII + H versus saline.

Fig.5 Relationship between L-type Ca^{2+} channel inhibition or K^+ sensitivity and systolic blood pressure. **a** Diltiazem concentration-relaxation curves of segments pre-constricted with 124 mM K^+ for saline- (open circles, white, n=6) and AngII-treated (solid circles, red or grey, n=12) mice or for AngII-treatment in combination with hydralazine (AngII + Hydra, solid circles, black, n=5). *, ***: P<0.05, 0.001 AngII versus control; $, $$, $$$: P<0.05, 0.01, 0.001 AngII + H versus AngII; #: AngII + H versus saline. **b** Window current induced contraction curves were determined by plotting the change of force (%) per mM change of extracellular K^+ for aortic segments in control (open circles, n=6) and following AngII-treatment (red or grey, solid circles, n=17) or AngII-treatment in combination with hydralazine (black, solid circles, n=5). *, **, ***: P<0.05, 0.01, 0.001 AngII versus saline; $, $$$: P<0.05, 0.01 AngII + H versus AngII; #, ###: P<0.05, 0.001 AngII + H versus saline. Relationship between the log(IC_{50}) of diltiazem (**c**)or EC_{50} of K^+ (**d**) and the systolic blood pressure of each animal. White (open) symbols refer to control animals, red or grey (solid) symbols to AngII-treated animals and black (solid) symbols to AngII-treated animals receiving hydralazine. Both linear relationships were significantly different from zero. The 95% confidence band is given by the dashed lines. Spearman r (Sr) and p are indicated in **c** and **d**.

Fig. 6 Effect of extracellular K^+ on isometric contractions of femoral artery segments of saline- and AngII-treated mice. **a** K^+ concentration-force curves for femoral artery segments in control (open circles) and following AngII-treatment (red, solid circles). For comparison the dashed lines indicate the K^+ concentration-force curves for aortic segments in control (black) and AngII (red). Window current induced contraction curves for femoral artery in control (**b**) and in the presence of 1 µM levcromakalim (**c**) were constructed by plotting the change of force (%) per mM change of extracellular K^+. The arrows in **b** show the shifts of the window current induced contraction curves in femoral artery (dashed lines) versus aorta, whereas in **c** they show the shifts of the window current induced contraction curves in femoral artery after addition of 1 µM levcromakalim. *, **, ***: $P<0.05$, 0.01, 0.001 AngII versus control; n=6 for control and n=6 for AngII

Fig. 7 AngII concentration-response curves for femoral artery and aorta**.** Force was measured for increasing AngII concentrations in control solution (open circles) and following mild depolarization with 20 (femoral artery, **a**) or 27.5 mM K^+ (aorta, **b**) (solid circles). AngII increased force in femoral artery at both K^+ concentrations, whereas in aortic segments, AngII was ineffective even after a slight increase of basal force with 27.5 mM K^+. **, ***: $P<0.01$, 0.001 high versus low K^+, n=3.

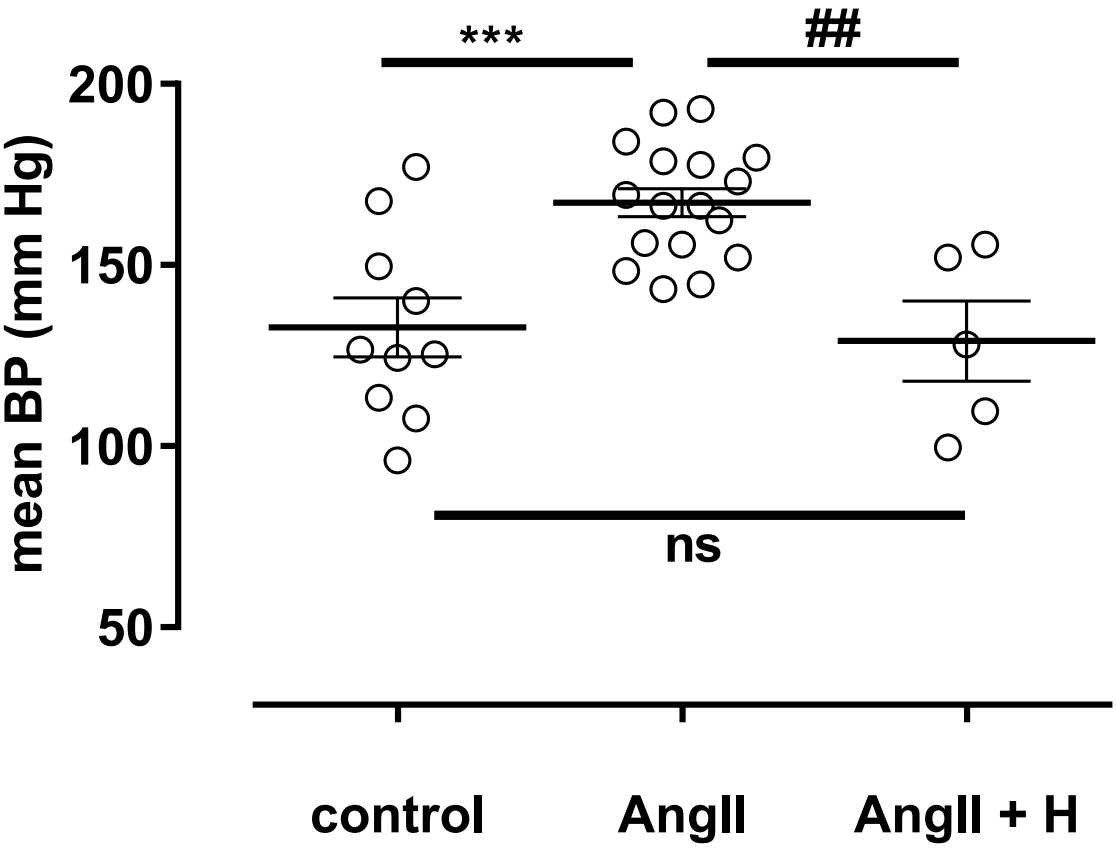
***
##
200
150
100
50
mean BP (mm Hg)
ns
control
AngII
AngII + H

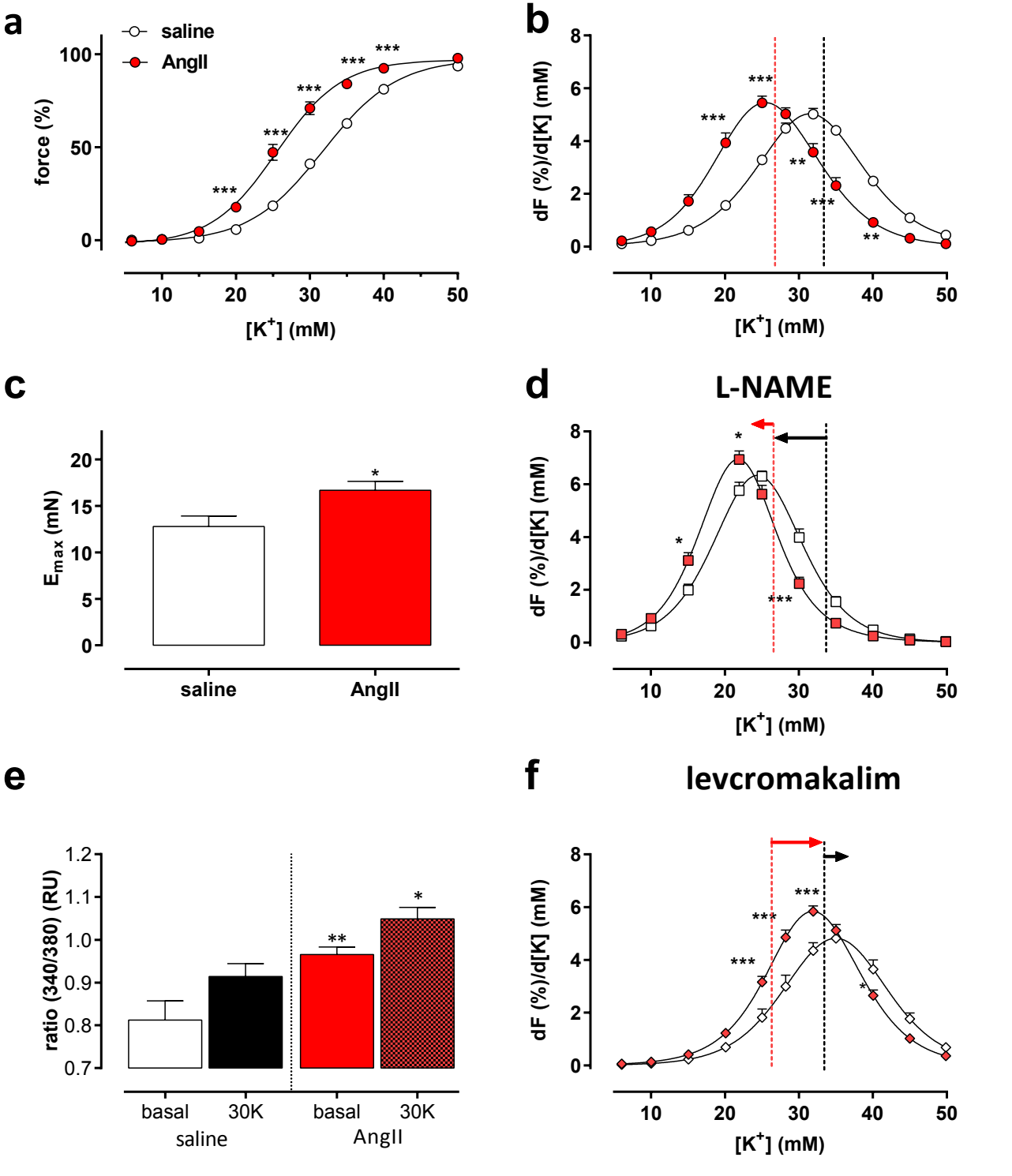
a
saline
AngII
force (%)
[K+] (mM)
b
dF (%)/d[K] (mM)
[K+] (mM)
c
Emax (mN)
saline
AngII
d
L-NAME
dF (%)/d[K] (mM)
[K+] (mM)
e
ratio (340/380) (RU)
basal
30K
basal
30K
saline
AngII
f
levcromakalim
dF (%)/d[K] (mM)
[K+] (mM)

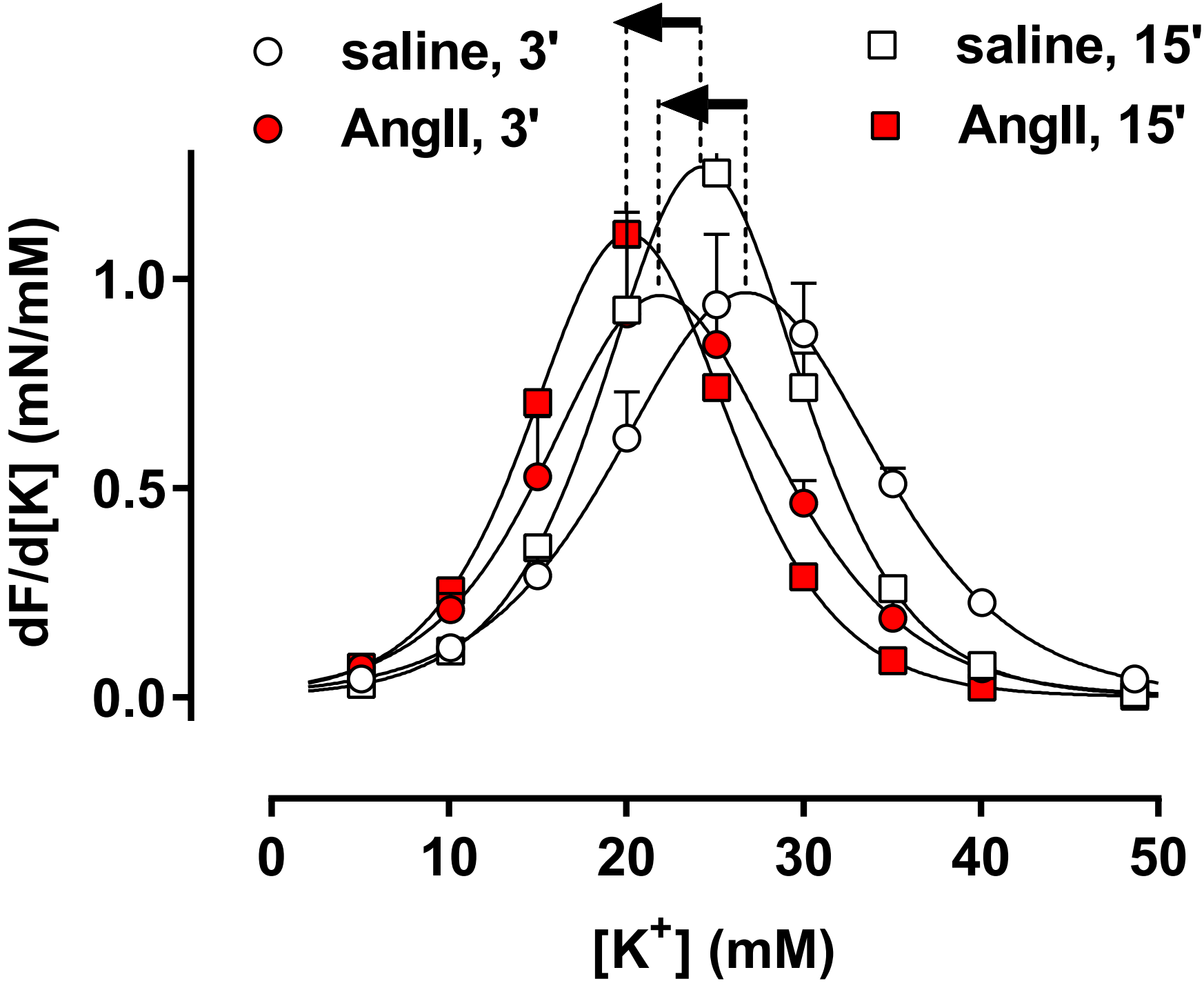
saline, 3'
AngII, 3'
saline, 15'
AngII, 15'
dF/d[K] (mN/mM)
1.0
0.5
0.0
0
10
20
30
40
50
[K+] (mM)

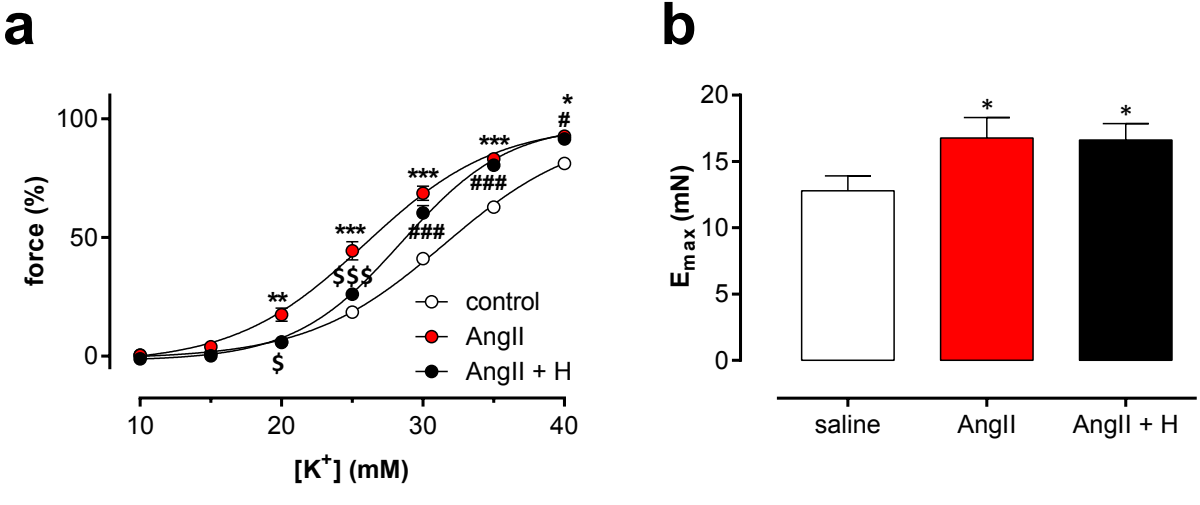
a
b
force (%)
100
50
0
10
20
30
40
[K+] (mM)
control
AngII
AngII + H
**
***
$
$$$
###
*
#
Emax (mN)
20
15
10
5
0
saline
AngII
AngII + H

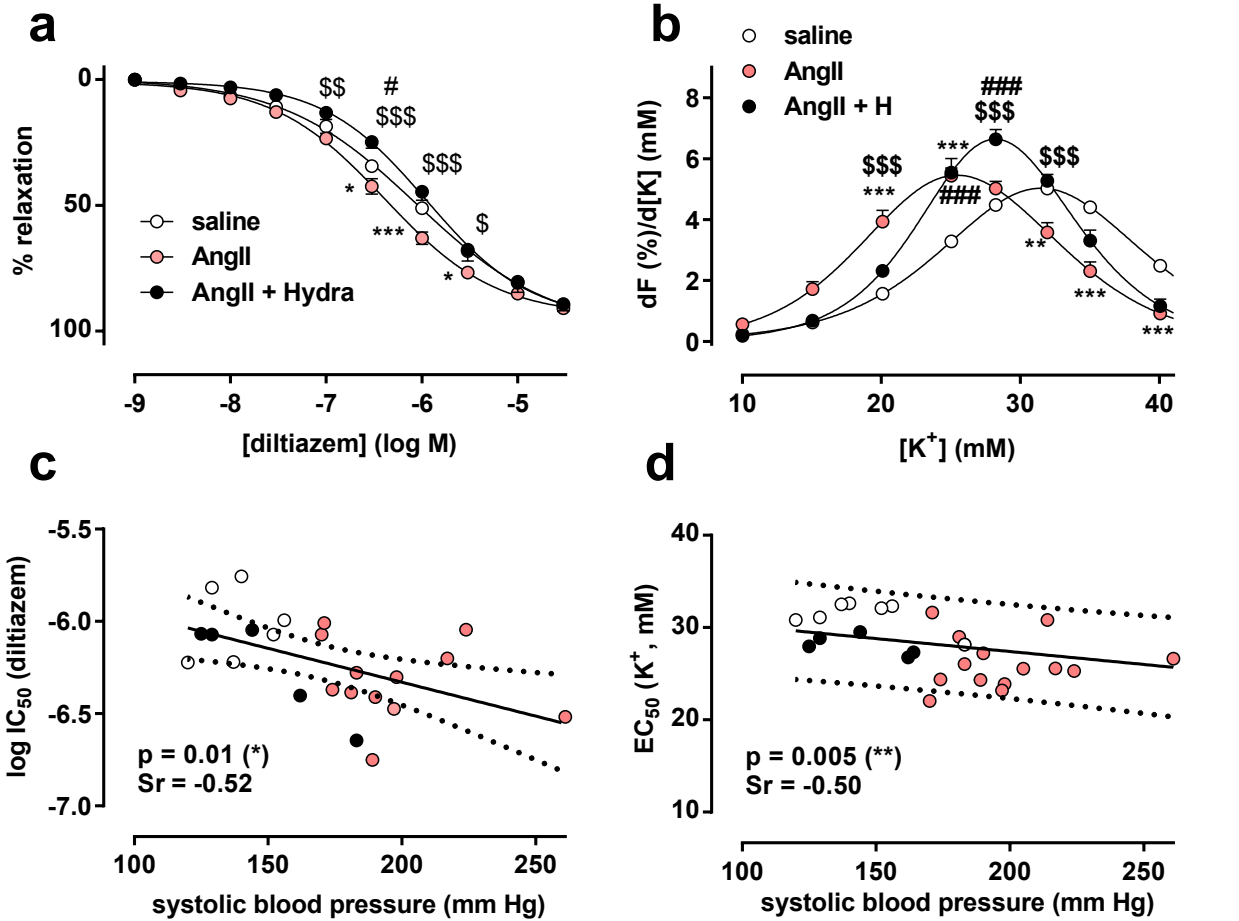
a
% relaxation
0
50
100
saline
AngII
AngII + Hydra
$$
#
$$$
$$$
$
*
***
*
-9
-8
-7
-6
-5
[diltiazem] (log M)
b
saline
AngII
AngII + H
dF (%)/d[K] (mM)
0
2
4
6
8
$$$
***
***
###
###
$$$
$$$
**
***
***
10
20
30
40
[K+] (mM)
c
log IC50 (diltiazem)
-5.5
-6.0
-6.5
-7.0
p = 0.01 (*)
Sr = -0.52
100
150
200
250
systolic blood pressure (mm Hg)
d
EC50 (K+, mM)
40
30
20
10
p = 0.005 (**)
Sr = -0.50
100
150
200
250
systolic blood pressure (mm Hg)

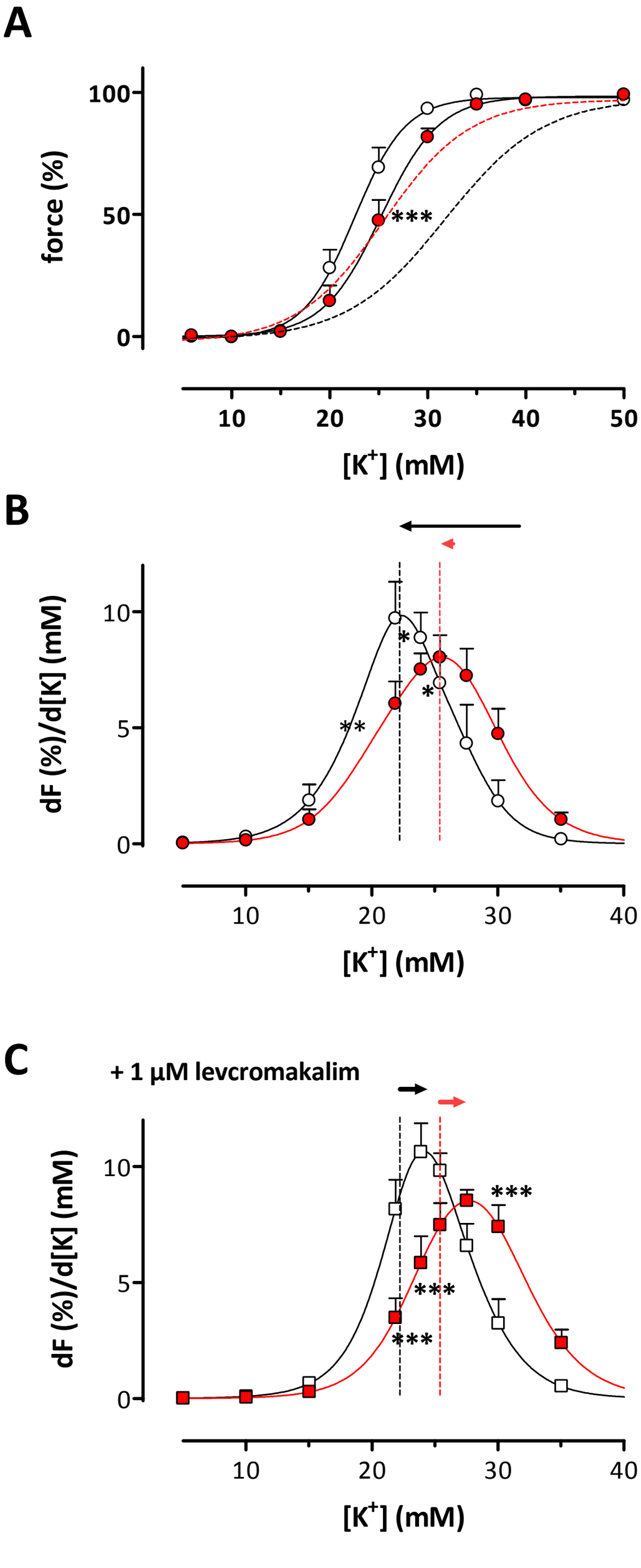
A
force (%)
100
50
0
***
10
20
30
40
50
[K+] (mM)
B
dF (%)/d[K] (mM)
10
5
0
**
*
*
10
20
30
40
[K+] (mM)
C
+ 1 µM levcromakalim
dF (%)/d[K] (mM)
10
5
0
***
***
***
10
20
30
40
[K+] (mM)

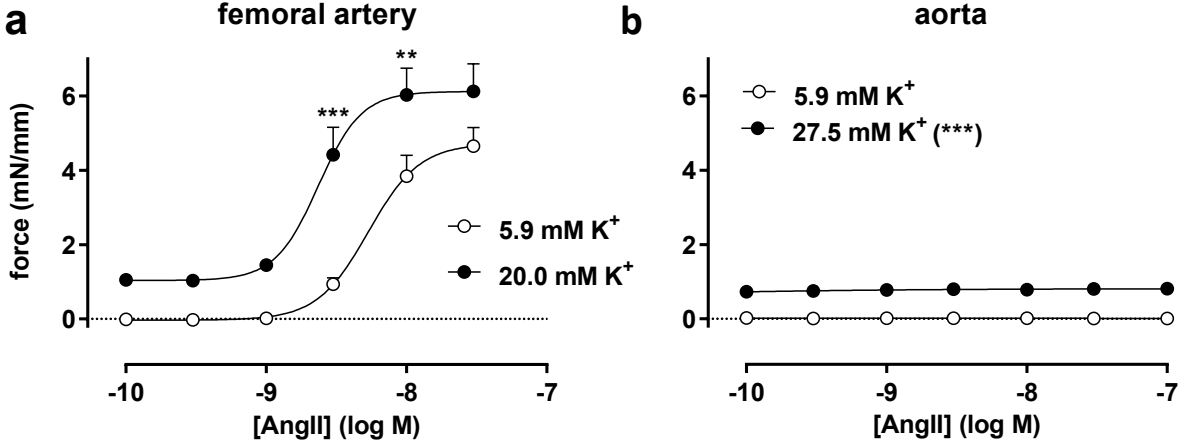
a
femoral artery
force (mN/mm)
6
4
2
0
**
***
5.9 mM K+
20.0 mM K+
-10
-9
-8
-7
[AngII] (log M)
b
aorta
6
4
2
0
5.9 mM K+
27.5 mM K+ (***)
-10
-9
-8
-7
[AngII] (log M)